The Aurora Kinase Inhibitor VX-680 Induces Endoreduplication and Apoptosis Preferentially in Cells with Compromised p53-Dependent Postmitotic Checkpoint Function

Farid Gizatullin,[1,2] Yao Yao,[4] Victor Kung,[1] Matthew W. Harding,[4] Massimo Loda,[1,3] and Geoffrey I. Shapiro[1,2]

[1]Department of Medical Oncology, Dana-Farber Cancer Institute; Departments of [2]Medicine and [3]Pathology, Brigham and Women's Hospital and Harvard Medical School, Boston, Massachusetts; and [4]Vertex Pharmaceuticals, Inc., Cambridge, Massachusetts

Abstract

VX-680 is a potent inhibitor of Aurora kinases that induces the accumulation of cells with ≥4N DNA content, followed by cell death. Here, we define the role of p53 and p21$^{Waf1/Cip1}$ in cell cycle perturbations following exposure to VX-680. Endoreduplication and apoptosis in response to VX-680 are limited in A549 and MCF-7 cells expressing wild-type p53, and markedly enhanced in cells lacking p53, including those engineered to express the HPV16-E6 oncoprotein or short interfering RNA pools targeting p53. In contrast, endoreduplication and apoptosis occur in the p53 wild-type cell lines, RKO and U2OS. The difference in response to VX-680 among these cell lines correlates with the timing of induction of p21$^{Waf1/Cip1}$ and its ability to inhibit cyclin E-cdk2 activity. In A549 cells, VX-680 induces the expression of p53 and p21$^{Waf1/Cip1}$ within 24 hours, with consequent inhibition of cyclin E-cdk2, and reduction of retinoblastoma protein phosphorylation, limiting endoreduplication. In RKO and U2OS cells, the induction of p21$^{Waf1/Cip1}$ is delayed and associated with higher residual cyclin E-cdk2 kinase activity and retinoblastoma protein phosphorylation, followed by progressive endoreduplication and apoptosis. Abrogation of p21$^{Waf1/Cip1}$ expression by short interfering RNA targeting in A549 cells results in a substantial increase in the degree of endoreduplication, whereas inducible expression of p21$^{Waf1/Cip1}$ in p53-negative NCI-H1299 cells inhibits VX-680-induced endoreduplication and cell death. These data suggest that the integrity of the p53-p21$^{Waf1/Cip1}$–dependent postmitotic checkpoint governs the response to Aurora kinase inhibition. Although cells with intact checkpoint function arrest with 4N DNA content, those with compromised checkpoint function are more likely to undergo endoreduplication followed by eventual apoptosis. (Cancer Res 2006; 66(15): 7668-77)

Introduction

The Auroras comprise a family of serine/threonine kinases that are essential for mitotic progression. The mammalian kinases, Aurora A, Aurora B, and Aurora C, share similar catalytic domains, but show different subcellular localization (1). Aurora A localizes to duplicated centrosomes and the spindle poles and participates in processes required for assembly of the spindle apparatus, including centrosome maturation and separation (2). In contrast, Aurora B is a chromosome passenger protein, localized to centromeres during prometaphase and relocated to the spindle midphase during anaphase onset (3). Aurora B is required for the phosphorylation of histone H3, chromosome segregation, and cytokinesis. Aurora C has also been shown to be a chromosome passenger protein that can complement Aurora B function and is required for cytokinesis (4, 5).

Aurora kinases are strongly associated with cancer. Overexpression of Aurora A transforms Rat1 and NIH/3T3 cells and gives rise to genetically unstable aneuploid cells with multiple centrosomes (6). Elevated expression has been detected in a high percentage of colon, breast, ovarian, gastric, and pancreatic tumors, and in a subset of these tumors, the AURKA locus (20q13) is amplified (7–10). Aurora B and Aurora C are also expressed at high levels in both primary tumors and cell lines (10). Levels of Aurora B have been shown to increase as a function of Duke stage in primary colon cancers (11). The expression of Aurora B often parallels that of Aurora A (7, 12).

To date, a growing number of inhibitors of Aurora kinases have been described (12) including Hesperadin (13), ZM447439 (14), and VX-680 (15). ZM447439 is an ATP-competitive inhibitor of Aurora A and Aurora B, whereas VX-680 inhibits all three family members (K$_i$'s of 0.6, 18 and 4.6 nmol/L for Aurora A, B, and C, respectively). VX-680 treatment results in cells with high levels of cyclin B1 and 4N DNA content 8 to 12 hours after release from a G$_1$-S block, indicating that cells can enter mitosis. The peak of cyclin B1 expression is slightly later in treated cells than in control cells, suggesting a delay in cell cycle progression. However, in VX-680-treated and control cultures, cyclin B1 expression subsequently decreases, indicating that mitotic exit is not blocked. After the completion of mitosis, control cells divide to yield daughters with 2N DNA content. In contrast, VX-680 induces the accumulation of cells arrested in a pseudo-G$_1$ state with a 4N DNA content or the accumulation of cells with >4N DNA content, the latter population representing cells that exit mitosis and subsequently proceed through S phase in the absence of cell division. Continued proliferation in the presence of aberrant mitosis and failed cytokinesis presumably results in cell death (15). ZM447439 and Hesperadin-treated cells both enter and exit mitosis with normal kinetics, demonstrating no effect on cell cycle progression, but similarly result in the accumulation of cells with 4N or >4N DNA content. The defective cytokinesis, as well as the inhibition of phosphorylation of histone H3 by all three drugs, suggests that the cellular effects of these agents might be largely mediated by the disruption of Aurora B function (12).

Whether cells arrest with 4N DNA content in pseudo-G$_1$ or endoreduplicate with the accumulation of >4N DNA content likely

depends on the integrity of the p53-dependent postmitotic checkpoint (16, 17). This checkpoint has been reported to induce the G_1 arrest of tetraploid cells that arise following mitotic errors including spindle disruption and cytokinetic failure, and involves p53-dependent induction of p21^Waf1/Cip1, resulting in the suppression of cdk2 activity (18, 19). There is current controversy over whether this postmitotic checkpoint is truly a "tetraploid checkpoint," because in some experimental systems, it is not triggered by tetraploidy, cytokinetic failure, or aberrant centrosome number (20–22). Nonetheless, p53 is frequently activated in tetraploid cells. In this way, p53 adds to the spindle checkpoint to prevent the propagation of cells with an abnormal genome. Consistent with the role of p53 in constraining endoreduplication following Aurora inhibition, the expression of dominant-negative p53 in U2OS osteosarcoma cells exaggerated the polyploidy induced by ZM447439 (14).

However, endoreduplication has been reported in response to ZM447439 and VX-680 in p53 wild-type cells (14, 15), suggesting that p53 status alone does not determine the response to Aurora inhibition. Furthermore, it has not yet been clarified whether cell death after exposure to Aurora kinase inhibitors depends on the absence of p53. To examine these issues further, we have explored the role of p53 in the response to VX-680. Here, we show that disruption of p53 function in wild-type A549 non–small cell lung cancer (NSCLC) cells causes increased endoreduplication after VX-680 treatment, followed by induction of apoptosis. However, in some p53 wild-type cells, including RKO colon carcinoma cells, endoreduplication is poorly constrained and is associated with cell death. In these cells, induction of p21^Waf1/Cip1 is delayed and suppression of cyclin E-cdk2 kinase activity and retinoblastoma (Rb) protein phosphorylation is incomplete. Furthermore, in A549 cells expressing short interfering RNA (siRNA) pools targeting p21^Waf1/Cip1, polyploidy is substantially increased, confirming the critical role of this cdk inhibitor in limiting endoreduplication. These data suggest that the overall integrity of the p53-p21^Waf1/Cip1 pathway in the G_1 postmitotic checkpoint governs the response to VX-680, and that cells with compromised checkpoint function are most likely to undergo apoptosis.

Materials and Methods

Cell culture. A549, Calu-1, NCI-H1299, SK-LU-1 and Calu-6 NSCLC, MCF-7 breast carcinoma, HeLa cervical carcinoma, RKO and RKO-E6 colon carcinoma, and U2OS osteosarcoma cell lines were obtained from the American Type Culture Collection and cultivated in the recommended medium. A549, MCF-7, RKO, and U2OS cells express wild-type p53. In Calu-1 and NCI-H1299 cells, *p53* is deleted; SK-LU-1 and Calu-6 cells carry *p53* mutations. A549 control and A549-E6 cells, generated via retroviral infection with LXSN or LXSN-HPV16E6, have been previously characterized and were maintained in medium supplemented with 400 μg/mL of G418 (23). In all instances, A549 parental cells and A549 LXSN cells behaved identically in response to VX-680.

Drug treatment. A 10 mmol/L stock of VX-680 was prepared in DMSO and stored at −20°C. Subconfluent cultures (5×10^5-10^6 cells per 10 cm dish) were seeded 24 hours prior to drug treatment. To assess the suppression of phosphorylation of histone H3 by VX-680, cells were first treated with 0.4 μg/mL of nocodazole (Sigma-Aldrich, Co., St. Louis, MO) for 16 hours followed by the addition of DMSO or drug for 3 hours (14).

Fluorescence-activated cell sorting analysis, bromodeoxyuridine analysis, and detection of apoptosis by flow cytometry. For cell cycle analysis, cells were analyzed for DNA content by flow cytometry using ModFit (Verity Software House, Topsham, ME) and CellQuest software (BD Biosciences, Franklin Lakes, NJ); the latter was used for quantification of

polyploidy. For bromodeoxyuridine (BrdUrd) analysis, the In situ Cell Proliferation Kit, FLUOS (Roche Applied Science, Indianapolis, IN) was used according to the manufacturer's protocol. Briefly, cells were pulse-labeled with 5-bromo-2′-deoxyuridine 1 hour before fixation, denaturation, and incubation with FITC-conjugated anti-BrdUrd antibody. Cells were stained with propidium iodide and analyzed by two-color flow cytometry. For apoptosis assays, a fluorescein apoptosis detection kit was used for terminal deoxynucleotidyltransferase (TdT)–mediated nick end labeling (TUNEL) assay (Promega, Madison, WI), as previously described (23). Following formaldehyde and ethanol fixation, pooled adherent and nonadherent cells were incubated with fluorescein-12 dUTP in the absence or presence of TdT, stained with propidium iodide and analyzed for DNA content and apoptosis using two-color flow cytometry. Apoptosis was quantified as the percentage of cells shifting to fluorescein-positivity in the presence of TdT, and was confirmed by Western blotting with an anti–cleaved PARP antibody (Cell Signaling Technology, Beverly, MA).

Protein extraction and Western blot analysis. Whole cell extracts were prepared in NP40 lysis buffer [50 mmol/L Tris-HCl (pH 8.0), 150 mmol/L NaCl, and 1% NP40], containing protease and phosphatase inhibitors (Calbiochem, San Diego, CA). In order to analyze the Rb protein, nuclear extraction was done using a nuclear extraction kit (Pierce, Rockford, IL) according to the manufacturer's protocol. For analysis of phosphohistone H3, cells were resuspended in radioimmunoprecipitation assay buffer [50 mmol/L Tris-HCl (pH 7.4), 150 mmol/L NaCl, 0.5% sodium deoxycholate, 1% NP40, and 0.1% SDS] and briefly sonicated twice. Protein concentration was determined using Bradford assay (Bio-Rad, Richmond, CA). Typically, 20 μg of cellular protein was subjected to SDS-PAGE and subsequent Western blotting using standard procedures, with the following primary antibodies: anti-p53, anti-p21^Waf1/Cip1, anti-Rb 4H1, anti-cyclin B1 V152 (all from Cell Signaling Technology); anti-β-actin (Sigma-Aldrich); anti-Ku70 (BD Transduction Laboratories, San Diego, CA); anti-cyclin E HE12 (Santa Cruz Biotechnology, Santa Cruz, CA); anti-Aurora A and anti-Aurora B (BD Biosciences PharMingen, San Jose, CA); and anti-phosphohistone H3 (ser10, clone 3H10; Upstate Biotechnology, Lake Placid, NY). Where indicated, bands were quantified using AlphaEase FC Software (Alpha Innotech Corp., San Leandro, CA).

Immunoprecipitation and histone H1 kinase assays. Cell lysates were prepared using protease and phosphatase inhibitors (Calbiochem) and subjected to immunoprecipitation with either anti-cyclin E HE111 or anti-cyclin B1 H433 antibodies (Santa Cruz Biotechnology). Immunoprecipitates were used to direct phosphorylation of exogenous histone H1 (Roche Applied Science) in the presence of 20 μmol/L of ATP and 10 μCi of [γ-^{33}P]ATP. Phosphorylated histone H1 was detected following SDS-PAGE, transfer to nitrocellulose, and exposure to X-ray film. Bands were quantified using AlphaEase FC Software (Alpha Innotech).

siRNA transfection. "Smart-pool" nonspecific oligos and those containing siRNA duplexes targeting Aurora A, Aurora B, p53, and p21^Waf1/Cip1 were obtained from Dharmacon, Inc. (Lafayette, CO). Cells were plated at 0.75×10^5 in six-well plates. Twenty-four hours later, transfection was done with 2 to 4 μL of OligofectAMINE (Invitrogen, Carlsbad, CA) using 50 nmol/L of the appropriate siRNA pools. In the analysis of combined Aurora A and B depletion, cells were collected 72 hours after transfection for flow cytometry and protein analyses. Forty-eight hours after transfection with p53 or p21^Waf1/Cip1 siRNAs, cells were replated and subsequently treated with VX-680 for 48 or 72 hours followed by flow cytometry and protein analyses.

Generation of NCI-H1299 cells inducibly expressing p21^Waf1/Cip1. The coding sequence of p21^Waf1/Cip1, derived from the plasmid containing the human cDNA clone (OriGene Technologies, Rockville, MD), was subcloned into pTRE-Hyg. The resulting construct was transfected into NCI-H1299 TetOn cells using Fugene 6 (Roche Applied Science). Clones were selected in 250 μg/mL of hygromycin (Invitrogen) and tested for inducible expression of p21^Waf1/Cip1 in the presence of doxycycline (Sigma-Aldrich). NCI-H1299 TetOn cells and the TRE2-Hyg plasmid were provided by Dr. Andrew Phillips (Medical College of Georgia, Augusta, GA).

Statistical analysis. Statistical analysis was done with the two-tailed, unpaired Student's t test. $P < 0.05$ was considered statistically significant.

Results

VX-680-induced endoreduplication is enhanced in the absence of p53 function. As shown in Fig. 1*A*, treatment of A549 p53 wild-type NSCLC cells with VX-680 induces the accumulation of cells with 4N and 8N DNA content, similar to that described with ZM447439 (14). The predominant effect of VX-680 at 24 hours is the accumulation of cells with 4N DNA content. However, at 48 hours, endoreduplication occurs in only a minority of cells, with ~20% demonstrating 8N DNA content (Fig. 2*B*). No further increase in the degree of polyploidy was observed up to 120 hours of drug exposure. In contrast, in A549 cells expressing the HPV16-E6 oncoprotein, in which p53 function is abrogated, endoreduplication is significantly enhanced at the 48-hour time point, with >50% of the population demonstrating 8N DNA content. In addition, endoreduplication continues with time, as evidenced by the appearance of cells with 16N DNA content at 72 hours and beyond (Fig. 1*A* and *B*). This is reflected in incorporation of BrdUrd in which pulse-labeling was done between 71 and 72 hours after VX-680 exposure; in A549 cells, there is a marked diminution in DNA synthesis, whereas in A549-E6 cells, DNA synthesis clearly continues, consistent with continued endoreduplication (Fig. 1*C*).

Enhanced endoreduplication induced by VX-680 in p53-negative cells is accompanied by loss of viability. Over time, in A549-E6 cells, cell death occurs, as shown by viable cell counts at the 72- and 96-hour time points (Fig. 1*D*). This is accompanied by the appearance of a sub-G_1 peak in the DNA content analysis (Fig. 1*A*), confirmed to represent apoptosis by TUNEL assay (Fig. 1*E* and *F*) and by assessment of PARP cleavage (Fig. 1*G*). In TUNEL assays, 8N and 16N most readily shifted to fluorescein positivity, suggesting that endoreduplicating cells were the most likely to undergo apoptosis (Fig. 1*F*). In contrast, in control cells, viability is maintained, and sub-G_1 DNA content, significantly increased TUNEL positivity, and PARP cleavage are not detected.
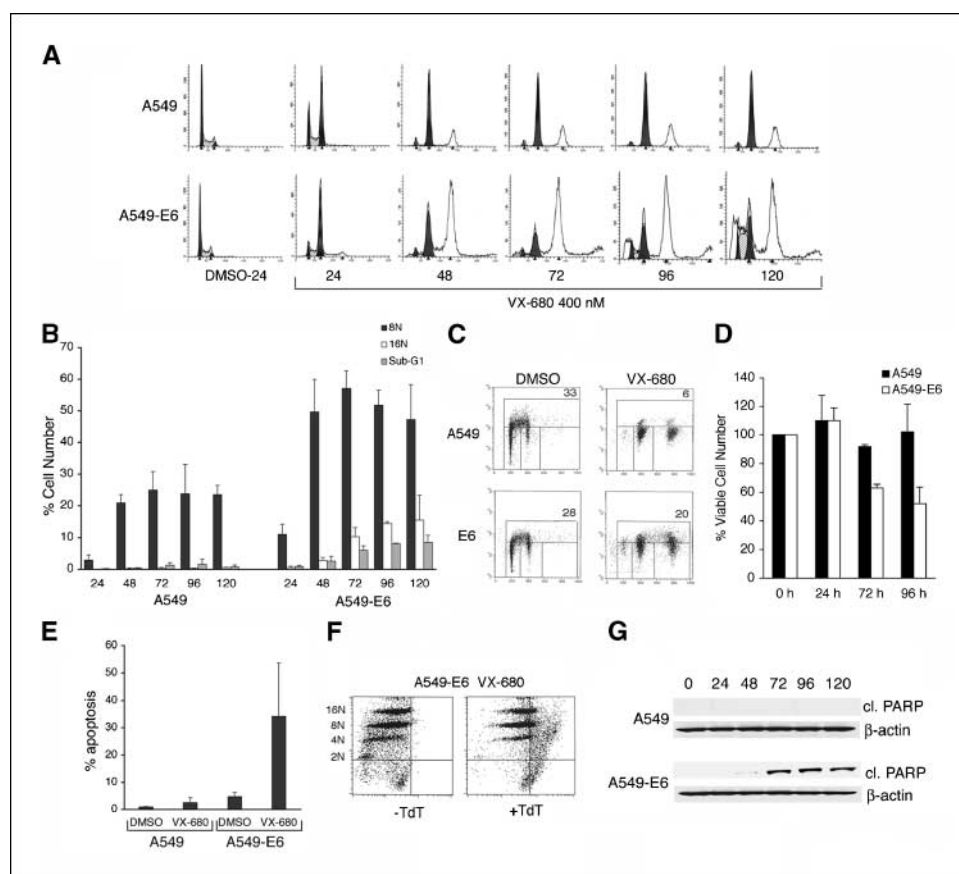
Figure 1. Abrogation of p53 function in A549 cells increases endoreduplication and apoptosis and translates to decreased cell viability. *A,* A549 parental and A549-E6 cells were treated with 400 nmol/L of VX-680 for the indicated times and DNA content was analyzed by flow cytometry, demonstrating increased endoreduplication in A549-E6 cells with a larger 8N peak and the development of a 16N peak at 72 hours. In addition, at late time points (96 and 120 hours), sub-G_1 DNA content is present in E6-expressing cells. *B,* quantification of 8N, 16N, and sub-G_1 DNA content over a minimum of three experiments for each condition. The difference in degree of endoreduplication between A549-E6 and parental cells reached statistical significance, comparing quantification of the percentage of cells with 8N DNA content at 48 hours (*P* = 0.036). *Bars,* SD. *C,* A549 and A549-E6 cells treated with DMSO or 400 nmol/L of VX-680 for 71 hours were pulsed with BrdUrd for 1 hour, stained with FITC-conjugated anti-BrdUrd antibody and propidium iodide and analyzed by two-color flow cytometry (*y*-axis, fluorescein; *x*-axis, propidium iodide). In A549 cells treated with VX-680, there is substantially less BrdUrd incorporation, whereas in A549-E6 cells, DNA synthesis clearly continues. *D,* cell viability as determined by trypan blue exclusion in cells treated with VX-680 for the indicated times over three experiments at each time point. For each cell line, cell counts were normalized to the count at time 0, which was considered as 100% viability. There were statistically significantly fewer viable E6-expressing cells compared with parental cells after 72 hours (*P* = 0.0000135) and 96 hours (*P* = 0.011) of VX-680 exposure. *Bars,* SD. *E,* analysis of apoptosis by TUNEL assay at 72 hours in cells treated with DMSO or VX-680. VX-680 induces significantly more apoptosis in A549-E6 cells compared with parental cells (*P* = 0.0085). *Columns,* mean average of two or three experiments, for DMSO or VX-680–treated cells, respectively; *bars,* SD. *F,* a representative TUNEL assay for A549-E6 cells treated with 400 nmol/L VX-680 for 72 hours (*y*-axis, fluorescein; *x*-axis, propidium iodide). The data show that 8N and 16N most readily shifted to fluorescein-positivity, suggesting that cells undergoing endoreduplication may be particularly prone to apoptosis. *G,* at the indicated times after treatment with 400 nmol/L VX-680, lysates were collected and subjected to Western blot analysis with the indicated antibodies, demonstrating cleavage of PARP in E6-expressing cells.
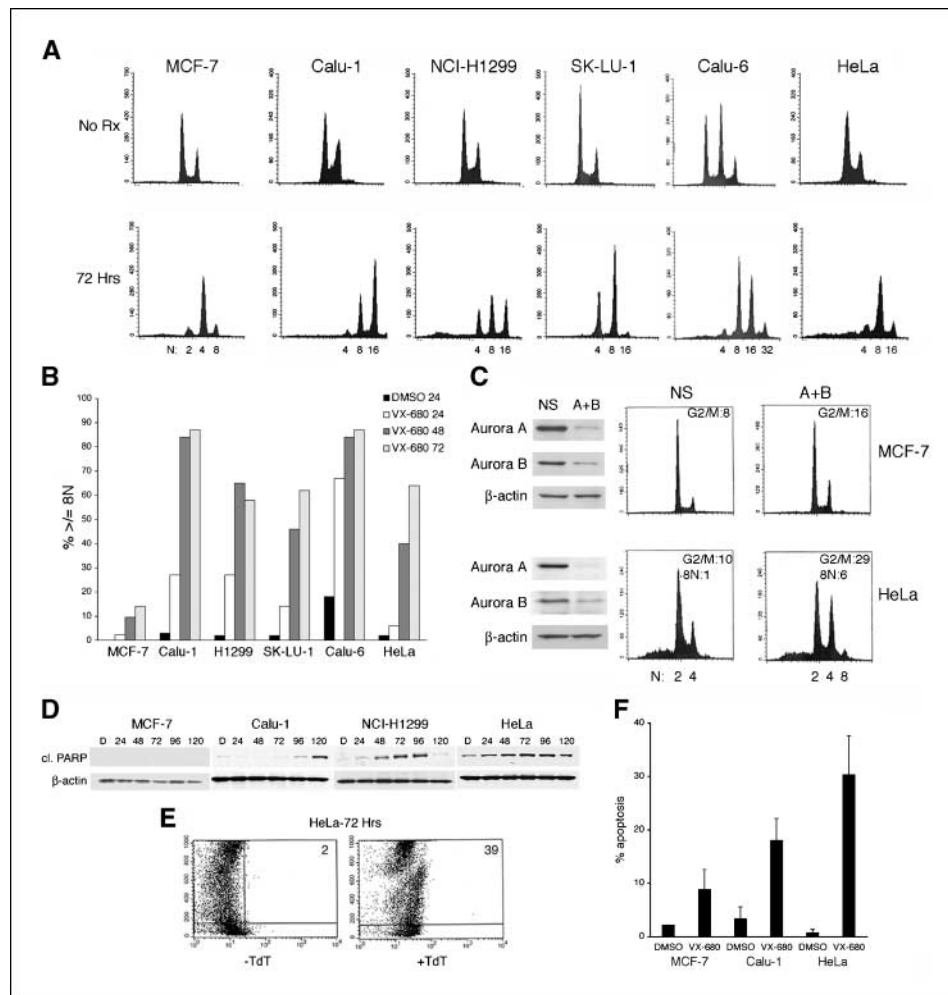
Figure 2. Endoreduplication and apoptosis occur readily in p53-negative cells after VX-680 exposure. *A,* MCF-7 (p53 wild-type), Calu-1, NCI-H1299, SK-LU-1, Calu-6, and HeLa cells (all p53-negative), were untreated or treated with 400 nmol/L VX-680 for 72 hours. DNA content was analyzed by flow cytometry. MCF-7 cells largely remain arrested with 4N DNA content with only a small amount of 8N present at 72 hours. In contrast, the other five cell lines show substantial endoreduplication. A cell population with sub-G$_1$ DNA content is most evident in NCI-H1299 and HeLa cells. *B,* quantification of polyploidy in the cell line panel examined in (*A*) treated with DMSO or 400 nmol/L of VX-680 for 24, 48, and 72 hours. MCF-7 cells show only a small degree of accumulation of 8N cells, whereas the other cell lines undergo substantial, progressive endoreduplication over the time course. *C,* MCF-7 and HeLa cells were treated with nonspecific RNAi (*NS*) or siRNA duplexes targeting both Aurora A and Aurora B together (*A + B*). After 72 hours, cells were subjected to Western blot and flow cytometry analyses. In MCF-7 cells, codepletion of Auroras increases the 4N DNA content without inducing endoreduplication. In contrast, HeLa cells show a higher degree of 4N DNA content along with endoreduplication. *D,* MCF-7, Calu-1, NCI-H1299, and HeLa cell lines were treated with 400 nmol/L of VX-680 for the indicated times and lysates were subjected to Western blot analysis, demonstrating PARP cleavage in the p53-negative cell lines. *E,* HeLa cells were treated with 400 nmol/L of VX-680 for 72 hours, fixed and subjected to TUNEL assay. Fluorescein is on the *x*-axis and propidium iodide staining is on the *y*-axis. The data show the shift to fluorescein positivity of polyploid cells, as well as cells with lower DNA content, including sub-G$_1$. *F,* MCF-7, Calu-1, and HeLa cells were treated with DMSO or 400 nmol/L of VX-680 for 72 hours, fixed and subjected to TUNEL assay. Compared with MCF-7 cells, the amount of apoptosis induced in Calu-1 ($P = 0.018$) and HeLa cells ($P = 0.0004$) was significantly greater. *Columns,* mean compilation of a minimum of three experiments in each VX-680-treated cell line; *bars,* SD.

These results were confirmed in several additional cell lines. MCF-7 cells also express wild-type 53 and behave similarly to A549 cells after VX-680 treatment. Over a 72-hour exposure, most cells are arrested with 4N DNA content, and only a small proportion show 8N DNA content (Fig. 2*A* and *B*). In contrast, substantial endoreduplication is detected 24 to 48 hours after VX-680 treatment in cells in which *p53* is deleted (Calu-1 and NCI-H1299), mutated (SK-LU-1 or Calu-6), or in which p53 is inactivated by HPV16E6 oncoprotein expression (HeLa). By 72 hours, 16N DNA content is apparent. These results are reflected in combined siRNA-mediated codepletion of Aurora A and Aurora B. In MCF-7 cells, this manipulation increases the 4N DNA content without inducing endoreduplication; in HeLa cells, the degree of increase of 4N DNA content is greater and endoreduplication is detected (Fig. 2*C*).

In MCF-7 cells, apoptosis is minimal, as detected by TUNEL assay (Fig. 2*F*) and confirmed by the absence of PARP cleavage (Fig. 2*D*). NCI-H1299 and HeLa cells show a greater proportion with sub-G$_1$ DNA content and DNA fragmentation than the other cell lines at the 72-hour time point (Fig. 2*A, E,* and *F*), indicating that loss of viability occurs more rapidly in some cell types than others. Nonetheless, evidence of PARP cleavage can be shown in other p53-negative cell lines as well, including Calu-1 (Fig. 2*D*).

Endoreduplication and apoptosis are readily detected in some p53 wild-type cell lines. RKO and U2OS cells also express wild-type p53. In contrast to the behavior of A549 and MCF-7 cells, in these cell lines, VX-680 causes progressive endoreduplication until 72 hours (with only a slight further increase at 96 hours) that is then followed by apoptosis (Fig. 3*A*). Similarly, siRNA-mediated

depletion of Aurora A and Aurora B together from U2OS cells results in the appearance of cells with 8N and sub-G_1 DNA content (Fig. 3B). Abrogation of p53 function still enhances the degree of endoreduplication and cell death, as shown by the analysis of RKO-E6 cells (Fig. 3C and D). Nonetheless, clearly not all cell lines expressing wild-type p53 respond to Aurora kinase inhibition with predominant 4N arrest and limited apoptosis.

Delayed p21$^{Waf1/Cip1}$ induction and persistent cyclin E-cdk2 activity with Rb phosphorylation occurs in response to VX-680 in RKO and U2OS cells. In order to ascertain why endoreduplication was more pronounced in RKO and U2OS cells than in A549 and MCF-7 cells, we examined components of the p53-dependent postmitotic checkpoint after 24 and 48 hours of exposure to VX-680. Figure 4A shows the induction of p53 after VX-680 treatment by 24 hours in all four of the cell lines, a response that persists at the 48-hour time point as well. In addition, at 24 hours, induction of p21$^{Waf1/Cip1}$ is robust in A549 and MCF-7 cells. In contrast, the induction of p21$^{Waf1/Cip1}$ is delayed in RKO and U2OS cells; at the 24-hour time point, there is only a slight increase in p21$^{Waf/Cip1}$ in RKO cells, whereas no increase is detected in U2OS cells until the 48-hour time point. The delay in p21$^{Waf1/Cip1}$

induction in RKO cells, compared with A549 cells, was confirmed in a more detailed time course over the first 48 hours of VX-680 exposure (Fig. 4D).

Consistent with differences in the timing of induction of p21$^{Waf1/Cip1}$ in these cell lines, the kinetics and degree of inhibition of cyclin E-cdk2 activity also differed. As shown in Fig. 4B, cyclin E-dependent kinase was reduced by ∼80% at 24 hours and 98% at 48 hours in A549 cells, the time point after which further endoreduplication is not detected. In contrast, cyclin E-dependent kinase activity is decreased by only 27% at 24 hours and 73% at 48 hours in RKO cells, accounting for continued endoreduplication observed at 72 hours in these cells. At the 72-hour time point, cyclin E-dependent kinase activity still persists in RKO cells, decreased by 93% (data not shown); between 72 and 96 hours, there is continued slight progression of endoreduplication (Fig. 3). These differences are also reflected in the degree of Rb phosphorylation after VX-680 exposure (Fig. 4A). In A549 cells and MCF-7 cells, Rb is largely dephosphorylated by 24 hours. In RKO and U2OS cells, phosphorylated Rb is detected at both the 24- and 48-hour time points, consistent with continued S phase entrance and endoreduplication. Finally, consistent with the arrest of cells with 4N
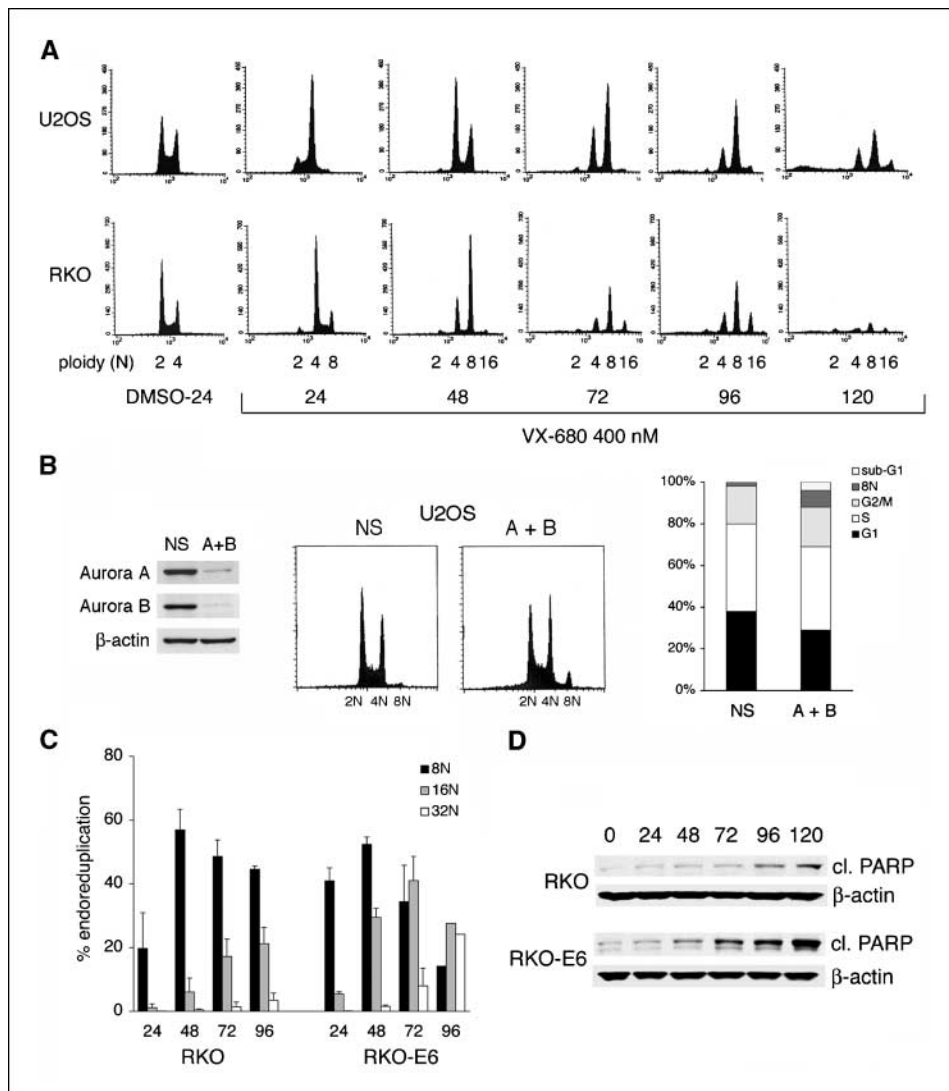

Figure 3. p53 wild-type RKO and U2OS cells undergo substantial endoreduplication in response to VX-680. *A,* cells were treated with DMSO or 400 nmol/L VX-680 for the indicated times. These data show that not all p53 wild-type cell lines behave identically in response to VX-680. RKO and U2OS cells, both of which express wild-type p53, undergo progressive endoreduplication until ∼72 hours, followed by eventual cell death in response to drug. *B,* U2OS cells were treated with nonspecific RNAi (*NS*) or siRNA duplexes targeting both Aurora A and Aurora B together (*A + B*). After 72 hours, cells were subjected to Western blot and flow cytometry analyses. *Bar graphs,* quantification of the cell cycle analysis. Codepletion of Auroras increases 4N DNA content, endoreduplication, and sub-G_1 DNA content in this cell line. *C,* disruption of p53 function in RKO-E6 cells increases endoreduplication in response to VX-680. RKO parental and RKO-E6 cells were treated with 400 nmol/L of VX-680 for the indicated times and DNA content was analyzed by flow cytometry. *Columns,* mean of a minimum of three experiments at each condition, except at 96 hours, where data represent the average of two or one experiment(s) for RKO and RKO-E6 cells, respectively; *bars,* SD. The degree of endoreduplication is statistically significantly greater in RKO-E6 cells, comparing the percentage of cells with 8N DNA content at 24 hours (*P* = 0.027) or 16N DNA content at 48 hours (*P* = 0.00049). *D,* at the indicated times after treatment with 400 nmol/L of VX-680, lysates were collected and subjected to Western blot analysis with the indicated antibodies, demonstrating enhanced cleavage of PARP in E6-expressing cells.
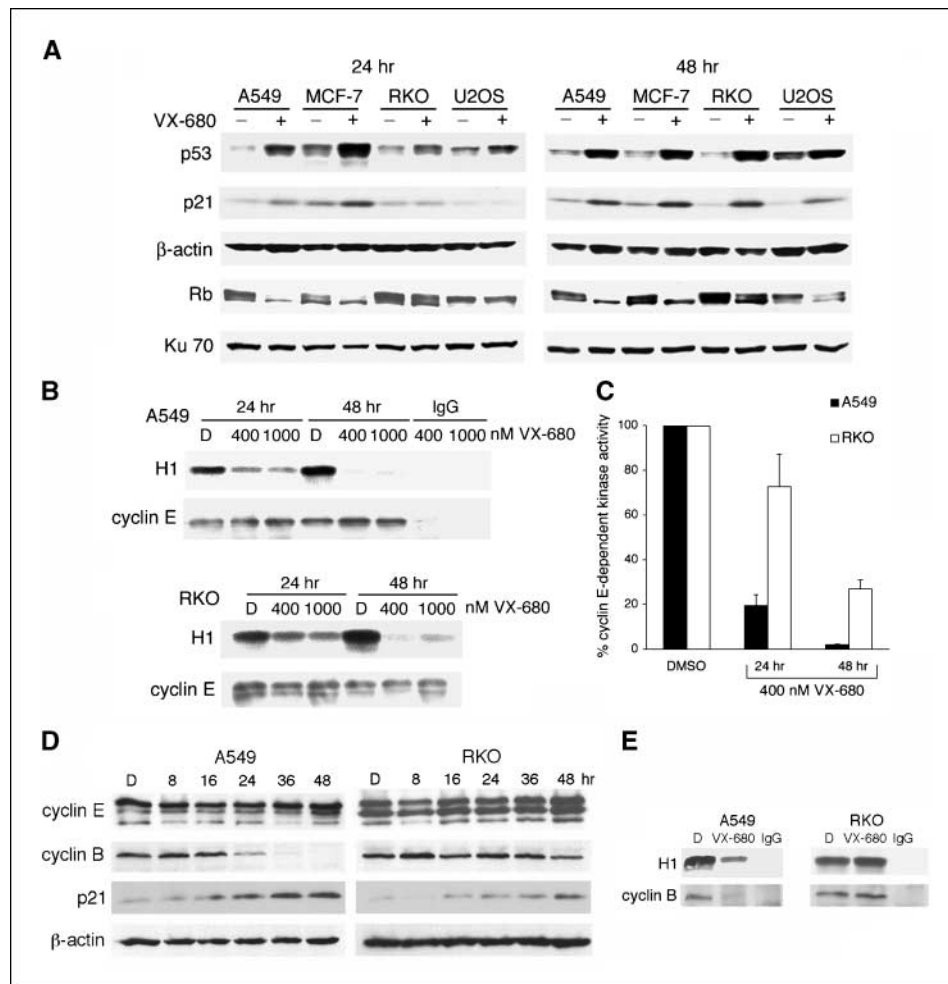
Figure 4. The degree of endoreduplication in p53 wild-type cell lines corresponds to the timing and amount of p21$^{Waf1/Cip1}$ induced, as well as to the degree of inhibition of cyclin E-cdk2. *A,* A549, MCF-7, RKO, and U2OS cells were treated with either DMSO or 400 nmol/L of VX-680 for 24 or 48 hours. Whole cell or nuclear lysates were subjected to Western blot analysis with the indicated antibodies. Nuclear lysates were used for analysis of the Rb protein; Western blotting for β-actin or Ku70 was used to show equal loading in whole cell and nuclear extracts, respectively. In A549 and MCF-7 cells, both p53 and p21$^{Waf1/Cip1}$ are induced after 24 hours, with a corresponding reduction in Rb phosphorylation. In RKO and U2OS cells, the induction of p21$^{Waf1/Cip1}$ is delayed, and is not detected until 48 hours after drug exposure. *B,* Cdk2 activity is diminished earlier and more completely in A549 cells compared with RKO cells following exposure to VX-680. A549 or RKO cells were treated with DMSO or the indicated concentrations of VX-680 for 24 or 48 hours. Lysates were subjected to immunoprecipitation with either IgG or anti-cyclin E antibodies followed by *in vitro* kinase assays in which immunoprecipitates were used to direct the phosphorylation of histone H1. Western blotting was used to show equal recovery of cyclin E in the assays. *C,* quantification of *in vitro* kinase assays in DMSO and VX-680-treated A549 and RKO cells. *Columns,* means of two experiments; *bars,* SD. The DMSO signal at 24 hours was considered to represent 100% activity for each cell line. There is significantly greater reduction in cyclin E-dependent kinase activity in A549 cells at 24 hours compared with RKO cells ($P = 0.039$). At 48 hours, there is only minimally detectable kinase activity in treated A549 cells, whereas kinase activity persists in RKO cells ($P = 0.012$). Consistent with the more rapid induction of p21$^{Waf1/Cip1}$, cdk2 activity was inhibited earlier in A549 cells, correlating with earlier cessation of endoreduplication. *D,* A549 and RKO cells were treated with DMSO or VX-680 400 nmol/L for the indicated times. Cell lysates were subjected to Western blot analysis using the indicated antibodies. The data confirm the delay in p21$^{Waf1/Cip1}$ induction in RKO cells compared with A549 cells over the first 48 hours of VX-680 exposure. Both cell lines show persistent cyclin E expression regardless of VX-680 treatment. However, A549 cells show decreased cyclin B expression during the time course of VX-680 exposure consistent with arrest of cell cycle progression. In contrast, cyclin B expression is not compromised in endoreduplicating RKO cells. *E,* cyclin B activity is diminished in A549 cells compared with RKO cells following exposure to VX-680. Cells were treated with DMSO or 400 nmol/L of VX-680 for 48 hours. Lysates were subjected to immunoprecipitation with either IgG or anti-cyclin B antibodies followed by *in vitro* kinase assays in which immunoprecipitates were used to direct the phosphorylation of histone H1. Western blotting was used to show the recovery of cyclin B, which is diminished in A549 cells arrested in pseudo-G$_1$. Cyclin B-dependent kinase activity is reduced ~ 70% in A549 cells and by <1% in RKO cells.

DNA content at the G$_1$-S boundary (pseudo-G$_1$ arrest), A549 cells show persistent cyclin E expression but decreased cyclin B expression after VX-680 exposure, reflected in a substantial diminution in cyclin B-dependent kinase activity (Fig. 4*D* and *E*). In contrast, in endoreduplicating RKO cells, cyclin B expression and cyclin B-dependent kinase activity are not compromised.

Induction of p21$^{Waf1/Cip1}$ correlates with suppression of endoreduplication in a concentration-dependent manner. As additional evidence that the amount of p21$^{Waf1/Cip1}$ induced after exposure to VX-680 correlates with the degree of endoreduplica-

tion that occurs, A549 cells were treated with a range of VX-680 concentrations. As shown in Fig. 5*A,* at 24 hours, there is a concentration-dependent increase in the amount of p21$^{Waf1/Cip1}$ induced. Full suppression of phosphohistone H3 phosphorylation in these cells is seen at VX-680 concentrations >200 nmol/L. At 48 hours after treatment with >200 nmol/L of VX-680, endoreduplication is constrained in a concentration-dependent manner, correlating with increased induction of p21$^{Waf1/Cip1}$ at higher concentrations (Fig. 5*B, bottom left*). The decrease in cells with 8N DNA content is accompanied by a reciprocal increase in the

percentage of cells with 4N DNA content, indicating more potent arrest in pseudo-G_1 at these concentrations. Similar data were obtained at 72 hours (data not shown). In contrast, the degree of endoreduplication plateaus and remains maximal irrespective of VX-680 concentration in A549-E6 cells (Fig. 5B, *bottom right*).

siRNA targeted depletion of p53 and p21$^{Waf1/Cip1}$ from A549 cells increases endoreduplication in response to VX-680. To further confirm the role of the p53-p21$^{Waf1/Cip1}$ pathway in constraining endoreduplication in response to VX-680, we used siRNA pools to transiently deplete these proteins from A549 cells. In the

absence of p53, there is progressive endoreduplication in response to 48 or 72 hours of VX-680 exposure, as was seen in A549 cells expressing the HPV16E6 oncoprotein (Fig. 6A and B). Endoreduplication after exposure to VX-680 for 48 hours is also substantial after depletion of p21$^{Waf1/Cip1}$ (Fig. 6A and B). This effect persists at the 72-hour time point. In the context of this experiment, progressive endoreduplication between 48 and 72 hours occurred but was slight, perhaps because of nonspecific induction of p53 after introduction of the siRNA targeting p21$^{Waf1/Cip1}$, limiting the depletion of p21$^{Waf1/Cip1}$ achieved over time (Fig. 6C).
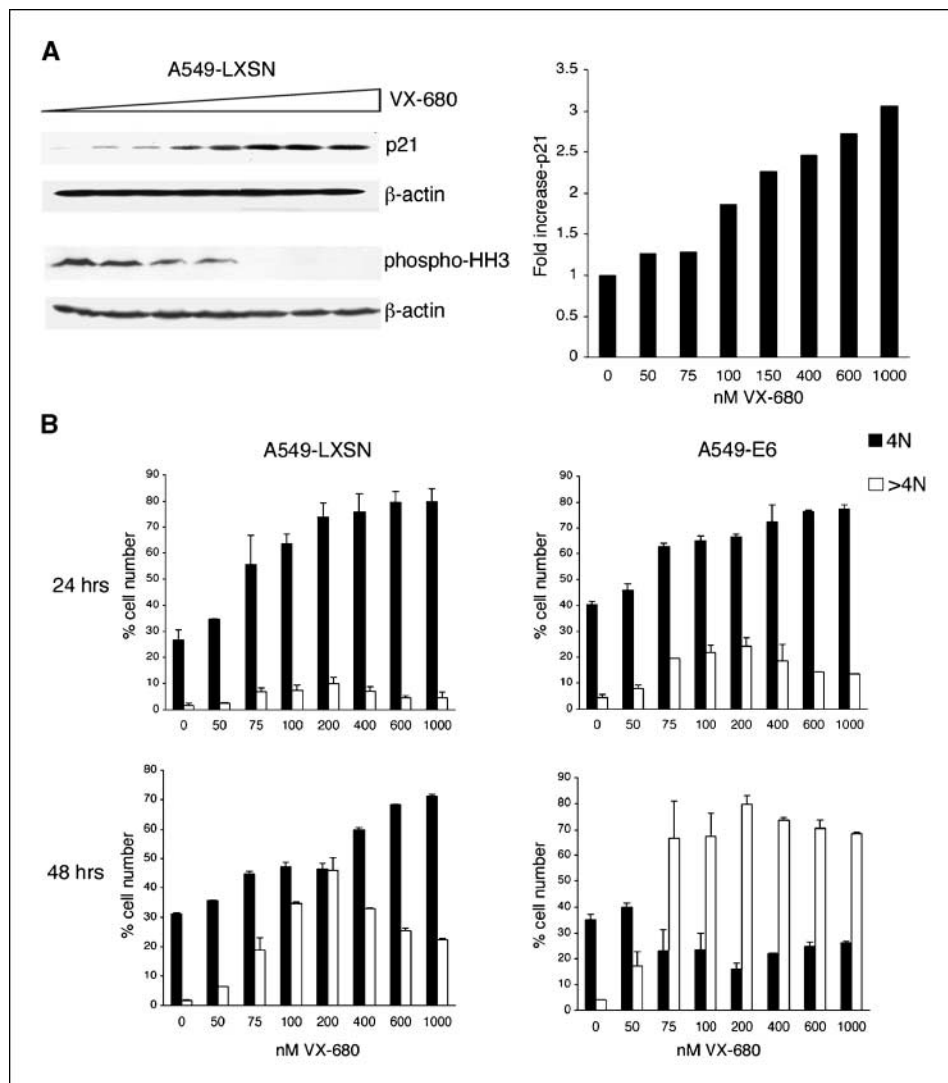
Figure 5. Concentration-dependent increase in p21$^{Waf1/Cip1}$ expression following VX-680 treatment correlates with constraint of endoreduplication in A549 cells. *A,* A549-LXSN cells were treated with DMSO or various concentrations of VX-680 ranging from 50 to 1,000 nmol/L for 24 hours. Lysates were subjected to Western blotting demonstrating a concentration-dependent increase in the expression of p21$^{Waf1/Cip1}$. Quantification of the p21$^{Waf1/Cip1}$ Western blot (*right*). In a second experiment, A549-LXSN cells were treated with nocodazole for 16 hours to induce mitotic arrest, followed by the addition of DMSO or 50, 100, 200, 400, 600, or 1,000 nmol/L of VX-680 for 3 hours. The data show that phosphorylation of histone H3 is fully suppressed at concentrations >200 nmol/L in these cells. *B,* A549-LXSN (*left*) and A549-E6 cells (*right*) were treated as in (*A*) for either 24 or 48 hours. Cells were collected at the indicated time points and DNA content was analyzed by flow cytometry. The percentage of cells with 4N DNA content and >4N DNA content are plotted. In the case of A549-LXSN cells, >4N denotes cells with 8N DNA content; in the case of A549-E6 cells, >4N denotes cells with either 8N or 16N DNA content. At 24 hours, there is a concentration-dependent increase in cells with 4N DNA content, plateauing at VX-680 concentrations ≥200 nmol/L in A549-LXSN cells. In both cell lines, the percentage of cells with >4N DNA content is limited at the 24 hours time point, although the degree of endoreduplication is greater in A549-E6 cells. At 48 hours, the two cell lines behave differently. Above concentrations ≥200 nmol/L, the percentage of A549-LXSN cells with 4N DNA content (likely representing pseudo-G_1) increases and the degree of endoreduplication decreases, correlating with increased induction of p21^{Waf1Cip1} at high concentrations. In A549-E6 cells, the degree of endoreduplication plateaus and remains maximal over a wide concentration range. The reduction in the degree of endoreduplication with increasing VX-680 concentration reached statistical significance in A549-LXSN cells (e.g., comparing 8N DNA content in cells treated with 200 or 600 nmol/L VX-680, *P* = 0.023). In contrast, no statistically significant differences in the degree of endoreduplication occurred across the concentrations tested in A549-E6 cells (for the same comparison, *P* = 0.1). *Columns,* mean average of two experiments; *bars,* SD.
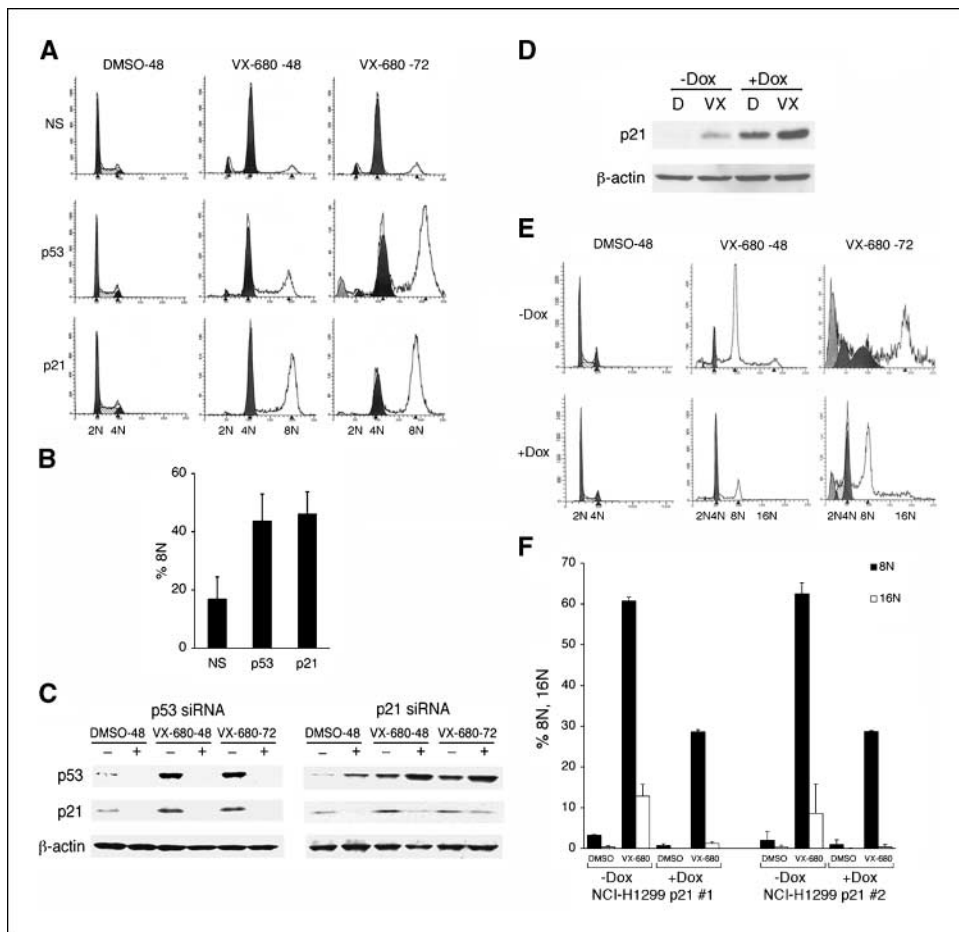
Figure 6. Endoreduplication is markedly enhanced in the absence of p53 or p21$^{Waf1/Cip1}$ and is limited by induction of p21$^{Waf1/Cip1}$ in p53-negative NCI-H1299 cells. *A,* nonspecific (NS) siRNAs or siRNAs targeting either p53 or p21$^{Waf1/Cip1}$ were introduced into A549 cells. 48 hours after transfection, cells were treated with DMSO or 400 nmol/L of VX-680 for an additional 48 or 72 hours. DNA content was analyzed by flow cytometry. *B,* the percentage of cells with 8N content following the introduction of the indicated siRNAs and subsequent treatment with 400 nmol/L of VX-680 for 48 hours is averaged for three experiments. There is a statistically significant increase in the degree of endoreduplication following depletion of either p53 ($P = 0.018$) or p21$^{Waf1/Cip1}$ ($P = 0.0092$) in A549 cells compared with cells treated with nonspecific siRNAs. *Bars,* SD. *C,* siRNA-mediated depletion of p53 and p21$^{Waf1/Cip1}$ was confirmed by Western blotting. *Left,* in cells treated with siRNAs targeting p53, both p53 and p21$^{Waf1/Cip1}$ are depleted, accounting for the progressive increase in endoreduplication observed at the 72-hour time point. *Right,* in cells treated with siRNAs targeting p21$^{Waf1/Cip1}$, along with the depletion of p21$^{Waf1/Cip1}$, there is an increase in p53 noted at 48 and 72 hours, affecting full depletion of p21$^{Waf1/Cip1}$ expression at 72 hours, perhaps accounting for the small increase in endoreduplication between 48 and 72 hours. *D,* a representative NCI-H1299 p21$^{Waf1/Cip1}$-inducible clone was treated with DMSO or (*D*) 400 nmol/L VX-680 (*VX*) in the presence or absence of doxycycline for 24 hours. Lysates were subjected to Western blot analysis, demonstrating strong induction of p21$^{Waf1/Cip1}$ in the presence of doxycycline. VX-680 treatment itself causes a small degree of p53-independent induction of p21$^{Waf1/Cip1}$. *E,* a representative NCI-H1299 p21$^{Waf1/Cip1}$-inducible clone was treated with DMSO or 400 nmol/L of VX-680 in the presence or absence of doxycycline for 48 and 72 hours, and analyzed by flow cytometry. In the absence of doxycycline, VX-680 induces a substantial fraction of cells with 8N and 16N DNA content. Cells with sub-G$_1$ DNA content are detected by 72 hours, suggesting the induction of apoptosis. In the presence of doxycycline, there is a sharp reduction in the degree of endoreduplication (at 48 and 72 hours) and the fraction of cells with sub-G$_1$ DNA content (72 hours). *F,* quantification of the percentage of cells with 8N and 16N DNA content in the absence or presence of doxycycline after 48 hours of VX-680 treatment is shown for this clone and for one additional clone. *Columns,* mean average of two experiments. For each clone, the total fraction of cells with ≥8N DNA content was significantly higher in the absence of doxycycline ($P = 0.0038$ and 0.0057 for clones 1 and 2, respectively).

Induction of p21$^{Waf1/Cip1}$ in p53-negative NCI-H1299 cells limits endoreduplication and cell death. Several NCI-H1299 p21$^{Waf1/Cip1}$-inducible clones were generated. Results for a representative clone are shown in Fig. 6*D* and *E*. In untreated cells, there is a strong induction of p21$^{Waf1/Cip1}$ in the presence of doxycycline (which is not detected in its absence). Interestingly, VX-680 treatment itself causes a small degree of p53-independent induction of p21$^{Waf1/Cip1}$ in these cells. Nonetheless, the amount of p21$^{Waf1/Cip1}$ induced is insufficient to prevent endoreduplication after 48 hours of drug exposure, with the appearance of a substantial percentage of cells with either 8N or 16N DNA content. In contrast, in the presence of doxycycline, the degree of endoreduplication is sharply reduced at the 48-hour time point. Quantification of cells with 8N or 16N DNA content in the absence or presence of doxycycline after

48 hours of VX-680 treatment is shown for this clone and for one additional clone in Fig. 6*F*. In the absence of doxycycline, cells with sub-G$_1$ DNA content are detected by 72 hours, consistent with the induction of apoptosis; the percentage of cells with sub-G$_1$ DNA content is substantially reduced in the presence of doxycycline (Fig. 6*E*).

Discussion

Aurora kinase inhibitors, including Hesperadin, ZM447439, and VX-680, all induce similar effects on cell division *in vitro*. The predominant outcome of exposure to these agents is not inhibition of cell cycle progression. Rather, following genome replication, drug-treated cells are able to enter and exit an aberrant mitosis,

with suppression of spindle checkpoint function. Because of failed cell division, tetraploidy results (12).

Following defective cytokinesis, the effect of longer exposure to Aurora kinase inhibition is cell line–dependent. Some cells undergo arrest in a pseudo-G_1 state, evidenced by a decrease in cyclin B in cells maintaining 4N DNA content, as shown in A549 cells (Fig. 4D). Other cells undergo additional rounds of DNA synthesis and with continued defective cytokinesis, develop polyploidy. Whether there is arrest in a tetraploid state or further endoreduplication most likely depends on the integrity of the postmitotic checkpoint (16, 17). This checkpoint is p53-dependent, although there is currently controversy over whether tetraploidy truly triggers this checkpoint and signals p53 activation (21). Nonetheless, induction of this checkpoint causes stable pseudo-G_1 arrest, as evidenced by the limited endoreduplication that occurs in A549 and MCF-7 cells beyond 48 hours, even with persistent exposure to VX-680 up to 120 hours. Consistent with the role of p53 in determining the degree of endoreduplication after Aurora kinase inhibition, expression of the HPV16E6 oncoprotein or siRNA pools targeting p53 in A549 cells results in a significantly greater degree of endoreduplication than that observed in parental cells.

However, the degree of endoreduplication in response to VX-680 is not governed by the presence of p53 alone. Some cell lines that express wild-type p53 still show substantial endoreduplication, including RKO and U2OS cells. We have shown that in these cell lines, there is a delay in the induction of $p21^{Waf1/Cip1}$. Because of this delay, at earlier time points (e.g., at 48 hours), the amount of $p21^{Waf1/Cip1}$ induced is insufficient to fully suppress cyclin E-cdk2 activity and Rb phosphorylation, permitting continued S phase entry and endoreduplication. In general, once maximal induction of $p21^{Waf1/Cip1}$ has occurred (24 hours in A549 and MCF-7 cells and 48 hours in RKO and U2OS cells), endoreduplication continues to progress for an additional 24 hours before there is >90% suppression of cyclin E-cdk2 activity with either no further increase or only minimal increase in polyploidy. Of note, the abrogation of p53 function in RKO cells permits progressive endoreduplication beyond 72 hours, whereas the degree of polyploidy remains minimally increased beyond this time point in parental cells (Fig. 3).

The importance of $p21^{Waf1/Cip1}$ in contributing to the constraint of endoreduplication was shown in experiments in which its level was modulated. In A549 cells, the amount of $p21^{Waf1/Cip1}$ induced by VX-680 is concentration-dependent. In the experiment shown in Fig. 5, the degree of endoreduplication observed is most likely the result of a balance between the potency of Aurora inhibition and the amount of $p21^{Waf1/Cip1}$ induced. At low concentrations (<200 nmol/L), there is probably insufficient $p21^{Waf1/Cip1}$ to fully restrict endoreduplication, and accumulation of cells with 8N DNA content increases with increasing concentrations of VX-680 and increasing degrees of Aurora inhibition. Above 200 nmol/L, Aurora inhibition is more complete, after which the amount of $p21^{Waf1/Cip1}$ continually increases, translating to a concentration-dependent limitation of endoreduplication. Further confirmation of the importance of $p21^{Waf1/cip1}$ in regulating the response to VX-680 was evidenced by the significant increase in endoreduplication observed in A549 cells when its expression was reduced by siRNA targeting and the reduced degree of endoreduplication that occurred when it was expressed in p53-negative NCI-H1299 cells.

It is not yet clear why the response of the p53-$p21^{Waf1/Cip1}$ pathway to VX-680 is not as robust in some cell lines. It is possible that there are other components of the p53 response after VX-680 exposure that must be intact for full postmitotic checkpoint function. These components might overlap with those of p53-dependent G_1 checkpoints induced after DNA damage or oncogene activation, including those that contribute to p53 stabilization such as chk2-mediated phosphorylation (24) or induction of $p14^{ARF}$ (25, 26). Other components might affect p53 activation, such as the ATM-dependent association of p53 with 14-3-3 proteins (27). The degree of p53 stability and activation likely contribute to the speed and abundance of $p21^{Waf1/cip1}$ that is ultimately induced. For example, U2OS cells have been reported to have low endogenous levels of chk2, and its ectopic expression enhances p53 stabilization and G_1 arrest in response to genotoxic stress (24). In this regard, use of VX-680 could help probe the role of proteins such as chk2 or $p14^{ARF}$ in the postmitotic checkpoint.

In the cell lines examined, the overall integrity of the p53-dependent postmitotic checkpoint governed not only the degree of endoreduplication but also the viability of cells exposed to VX-680. Flow cytometry-based TUNEL assays routinely showed fluorescein shift of polyploid cells (Figs. 1F and 2E; data not shown), suggesting that mitotic catastrophe (28) and DNA fragmentation following endoreduplication results in cells with variable DNA content, including sub-G_1 DNA content.

In some cell lines, endoreduplication proceeded longer, prior to the onset of cell death, whereas in other cell lines, the induction of apoptosis was faster. As shown in Fig. 2, Calu-1 cells continue to endoreduplicate with a substantial 16N peak at 72 hours; in HeLa cells, death is more abrupt, so that there is a smaller 16N peak and more cells with sub-G_1 DNA content. HeLa cells were among the most sensitive of the cell lines we studied. Importantly, these cells lack both functional Rb and p53. Rb also plays an important role in the postmitotic checkpoint (16, 29–31), and it will be of interest to more rigorously study whether loss of both Rb and p53 synergize in the induction of endoreduplication and eventual cell death.

As cells with a compromised p53-$p21^{Waf1/Cip1}$ pathway are more likely to die in response to VX-680, there is promise that Aurora inhibition will be selectively cytotoxic to malignant cells. Further work will be necessary to confirm that both normal fibroblasts and normal epithelial cells undergo pseudo-G_1 arrest without cell death in response to VX-680. In addition, short exposures to the drug may result in reversible effects in nontransformed cells and progressive endoreduplication and commitment to cell death in malignant cells. It is encouraging that there was little VX-680-induced toxicity in nude mice or rats harboring colon carcinoma or leukemia xenografts treated at concentrations that induced tumor growth inhibition and regression (15).

Because VX-680 inhibits all three Auroras, it is not yet clear which kinase is the primary target for antitumor activity. The effects of VX-680 most closely mirror those described for the siRNA-mediated depletion of Aurora B or combined depletion of Aurora A and Aurora B (32, 33). In both cases, there is an override of the spindle checkpoint, completion of and exit from an aberrant mitosis, with defective cytokinesis leading to polyploidy. In addition, in VX-680 cells, inhibition of tumor growth is paralleled by a reduction in histone H3 phosphorylation, an event attributed to Aurora B inhibition.

In contrast, the spindle checkpoint is effectively engaged following siRNA-mediated depletion of Aurora A alone in HeLa and U2OS cells (34). Therefore, it is unlikely that Aurora A inhibition alone could account for the effects of VX-680. Nonetheless, Aurora A depletion does delay mitotic entry, which has been described for VX-680, and causes failure of multiple mitotic events including separation of centriole pairs, misalignment of chromosomes on

the metaphase plate, and incomplete cytokinesis (2). Therefore, it is possible that the combined inhibition of Aurora A and Aurora B by VX-680 is critical for its antitumor effects.

The effects of VX-680 on cell lines possessing variable degrees of postmitotic checkpoint competency were reflected with siRNA-mediated codepletion of Aurora A and Aurora B in our experiments. In MCF-7 cells, combined depletion or depletion of Aurora A alone induced comparable increases in G_2-M DNA content without endoreduplication (Fig. 2C; data not shown); depletion of Aurora B alone caused a slight increase in G_2-M DNA content, again without endoreduplication (data not shown). In contrast, in postmitotic checkpoint–compromised U2OS cells, increases in G_2-M and 8N DNA content after combined Aurora A and Aurora B depletion were generally more apparent than with depletion of either alone (data not shown), as previously reported (33). Similarly, combined depletion reflects the effects of VX-680 in HeLa cells; endoreduplication after combined depletion in these cells is also greater than after depletion of Aurora B alone (33). However, the effects of combined depletion were overall not as dramatic as those induced by drug. This could be related to the incomplete suppression of expression by the siRNA duplexes. Alternatively, VX-680 also targets Aurora C, the activity of which should not be affected in siRNA-depleted cells. It has recently been shown that Aurora C can complement Aurora B function in mitotic cells, and that depletion of Aurora C

also leads to polyploidy (4, 5), so that Aurora C inhibition may also be contributing to the antitumor effects of VX-680.

VX-680 has recently entered clinical trials, and an increasing number of compounds will likely join this novel antineoplastic class. If the potential for selective antitumor cytotoxicity is met, further assessment of the critical Auroras necessary to inhibit for antitumor activity, as well as their interacting proteins, will guide new drug development. Finally, our data suggest that further dissection of the components of the postmitotic G_1 checkpoint may help select patient populations most likely to respond to Aurora kinase inhibition.

Acknowledgments

References

1. Carmena M, Earnshaw WC. The cellular geography of aurora kinases. Nat Rev Mol Cell Biol 2003;4:842–54.
2. Marumoto T, Zhang D, Saya H. Aurora A—a guardian of poles. Nat Rev Cancer 2005;5:42–50.
3. Adams RR, Carmena M, Earnshaw WC. Chromosomal passengers and the (aurora) ABCs of mitosis. Trends Cell Biol 2001;11:49–54.
4. Sasai K, Katayama H, Stenoien DL, et al. Aurora-C kinase is a novel chromosomal passenger protein that can complement Aurora-B kinase function in mitotic cells. Cell Motil Cytoskeleton 2004;59:249–63.
5. Yan X, Cao L, Li Q, et al. Aurora C is directly associated with Survivin and required for cytokinesis. Genes Cells 2005;10:617–26.
6. Zhou H, Kuang J, Zhong L, et al. Tumour amplified kinase STK15/BTAK induces centrosome amplification, aneuploidy and transformation. Nat Genet 1998;20:189–93.
7. Bischoff JR, Anderson L, Zhu Y, et al. A homologue of Drosophila aurora kinase is oncogenic and amplified in human colorectal cancers. EMBO J 1998;17:3052–65.
8. Sen S, Zhou H, White RA. A putative serine/threonine kinase encoding gene BTAK on chromosome 20q13 is amplified and overexpressed in human breast cancer cell lines. Oncogene 1997;14:2195–200.
9. Warner SL, Bearss DJ, Han H, Von Hoff DD. Targeting Aurora-2 kinase in cancer. Mol Cancer Ther 2003;2:589–95.
10. Katayama H, Brinkley WR, Sen S. The Aurora kinases: role in cell transformation and tumorigenesis. Cancer Metastasis Rev 2003;22:451–64.
11. Katayama H, Ota T, Jisaki F, et al. Mitotic kinase expression and colorectal cancer progression. J Natl Cancer Inst 1999;91:1160–2.
12. Keen N, Taylor S. Aurora-kinase inhibitors as anticancer agents. Nat Rev Cancer 2004;4:927–36.
13. Hauf S, Cole RW, LaTerra S, et al. The small molecule Hesperadin reveals a role for Aurora B in correcting kinetochore-microtubule attachment and in maintaining the spindle assembly checkpoint. J Cell Biol 2003; 161:281–94.
14. Ditchfield C, Johnson VL, Tighe A, et al. Aurora B couples chromosome alignment with anaphase by targeting BubR1, Mad2, and Cenp-E to kinetochores. J Cell Biol 2003;161:267–80.
15. Harrington EA, Bebbington D, Moore J, et al. VX-680, a potent and selective small-molecule inhibitor of the Aurora kinases, suppresses tumor growth *in vivo*. Nat Med 2004;10:262–7.
16. Margolis RL, Lohez OD, Andreassen PR. G1 tetraploidy checkpoint and the suppression of tumorigenesis. J Cell Biochem 2003;88:673–83.
17. Andreassen PR, Lohez OD, Margolis RL. G2 and spindle assembly checkpoint adaptation, and tetraploidy arrest: implications for intrinsic and chemically induced genomic instability. Mutat Res 2003;532:245–53.
18. Lanni JS, Jacks T. Characterization of the p53-dependent postmitotic checkpoint following spindle disruption. Mol Cell Biol 1998;18:1055–64.
19. Stewart ZA, Leach SD, Pietenpol JA. p21Waf1/Cip1 inhibition of cyclin E/Cdk2 activity prevents endoreduplication after mitotic spindle disruption. Mol Cell Biol 1999;19:205–15.
20. Stukenberg PT. Triggering p53 after cytokinesis failure. J Cell Biol 2004;165:607–8.
21. Uetake Y, Sluder G. Cell cycle progression after cleavage failure: mammalian somatic cells do not possess a "tetraploidy checkpoint." J Cell Biol 2004;165: 609–15.
22. Wong C, Stearns T. Mammalian cells lack checkpoints for tetraploidy, aberrant centrosome number, and cytokinesis failure. BMC Cell Biol 2005;6:6.
23. Shapiro GI, Koestner DA, Matranga CB, Rollins BJ. Flavopiridol induces cell cycle arrest and p53-independent apoptosis in non-small cell lung cancer cell lines. Clin Cancer Res 1999;5:2925–38.
24. Chehab NH, Malikzay A, Appel M, Halazonetis TD. Chk2/hCds1 functions as a DNA damage checkpoint in G(1) by stabilizing p53. Genes Dev 2000;14:278–88.
25. Sherr CJ. Tumor surveillance via the ARF-p53 pathway. Genes Dev 1998;12:2984–91.
26. Khan SH, Moritsugu J, Wahl GM. Differential requirement for p19ARF in the p53-dependent arrest induced by DNA damage, microtubule disruption, and ribonucleotide depletion. Proc Natl Acad Sci U S A 2000; 97:3266–71.
27. Waterman MJ, Stavridi ES, Waterman JL, Halazonetis TD. ATM-dependent activation of p53 involves dephosphorylation and association with 14-3-3 proteins. Nat Genet 1998;19:175–8.
28. Castedo M, Perfettini JL, Roumier T, Andreau K, Medema R, Kroemer G. Cell death by mitotic catastrophe: a molecular definition. Oncogene 2004;23:2825–37.
29. Niculescu AB III, Chen X, Smeets M, Hengst L, Prives C, Reed SI. Effects of p21Cip1/Waf1 at both the G1/S and the G2/M cell cycle transitions: pRb is a critical determinant in blocking DNA replication and in preventing endoreduplication. Mol Cell Biol 1998;18: 629–43.
30. Khan SH, Wahl GM. p53 and pRb prevent rereplication in response to microtubule inhibitors by mediating a reversible G1 arrest. Cancer Res 1998;58:396–401.
31. Borel F, Lohez OD, Lacroix FB, Margolis RL. Multiple centrosomes arise from tetraploidy checkpoint failure and mitotic centrosome clusters in p53 and RB pocket protein-compromised cells. Proc Natl Acad Sci U S A 2002;99:9819–24.
32. Giet R, Petretti C, Prigent C. Aurora kinases, aneuploidy and cancer, a coincidence or a real link? Trends Cell Biol 2005;15:241–50.
33. Yang H, Burke T, Dempsey J, et al. Mitotic requirement for aurora A kinase is bypassed in the absence of aurora B kinase. FEBS Lett 2005;579:3385–91.
34. Marumoto T, Honda S, Hara T, et al. Aurora-A kinase maintains the fidelity of early and late mitotic events in HeLa cells. J Biol Chem 2003;278:51786–95.